Stabilization of Linear Continuous-Time Systems using Neuromorphic Vision Sensors

Prince Singh [a,⋆] Sze Zheng Yong [a,⋆] Jean Gregoire [a] Andrea Censi [a] Emilio Frazzoli [a]

***Abstract*— Recently developed neuromorphic vision sensors have become promising candidates for agile and autonomous robotic applications primarily due to, in particular, their high temporal resolution and low latency. Each pixel of this sensor independently fires an asynchronous stream of "retinal events" once a change in the light field is detected. Existing computer vision algorithms can only process periodic frames and so a new class of algorithms needs to be developed that can efficiently process these events for control tasks. In this paper, we investigate the problem of *quadratically* stabilizing a continuous-time linear time invariant (LTI) system using measurements from a neuromorphic sensor. We present an H_∞ controller that stabilizes a continuous-time LTI system and provide the set of stabilizing neuromorphic sensor based cameras for the given system. The effectiveness of our approach is illustrated on an unstable system.**

I. Introduction

The output of a neuromorphic vision sensor is a sequence of events rather than periodic frames produced by a regular camera (e.g., CCD-, CMOS-based). We term these events as "retinal events" since they are generated once the observed light field changes by more than a user-chosen threshold [1].

The Dynamic Vision Sensor (DVS) is the first commercially available neuromorphic vision sensor [2] whose pixels independently and asynchronously fire retinal events once a change in the light field is detected. One big advantage of the DVS is that these retinal events are information bearing and so one avoids processing redundant data as with camera frames. In addition, the DVS has alluring properties, for example, micro-second temporal resolution, low-latency (order of micro-seconds) resulting in increased reactivity, high dynamic range ($> 120dB$) and low power requirement, collectively making it a viable sensor for enabling the quick computation of control commands to facilitate aggressive maneuvers of agile robots.

Literature Review. At the current state of the art, almost all vision based control of mobile robots rely on algorithms that are developed to process the frames from 'regular' cameras. These algorithms are unfortunately not suited to process the output of the low-latency neuromorphic vision sensors, which fire a sequence of asynchronous time-stamped events that describe a change in the perceived brightness at each pixel. In view of the DVS' interesting properties, this sensor seems to be an ideal choice for tasks that are limited by the sensing speed and/or the sensing power; for example, tasks ranging from stabilizing the upright position of robotic insects [3] to enabling high speed collision-free flights of autonomous micro-aerial vehicles in complex environments [4] (not achieved yet). Other existing works use neuromorphic vision sensors for balancing an inverted pencil [5] and for controlling an autonomous goalie [6]. The works in [7], [8] consider noisy events by modeling their generation through suitable noise processes. For example, [8] models ambiguities in the generation of the retinal events through a diffusion process deriving its inspiration from works that model the event activity in biological neurons. Furthermore, a proportional-derivative control scheme based on the DVS' ambiguous measurements was presented in [7] for the task of heading regulation. However, all the proposed methods are problem-specific and they involve first computing explicit representations for the states and then using these estimates for closed-loop control. Hence, it remains an open problem to consider if less restrictive conditions on a given system can be achieved by going directly from the events to control commands rather than performing control via state-estimation.

Additionally, one cannot readily apply existing control techniques developed in the event-based control literature [9], in which one typically has the flexibility to design a sensor (thus, events) to guarantee some performance requirement for the overall system (e.g., minimize the attention needed by the plant). However, in our case, we are given a sensor and are restrained by its inherent properties (i.e., with no means of controlling the retinal events except threshold design) to facilitate our control task.

Contributions. To the best of the authors' knowledge, this work is the first to address the stability of a continuous time linear time invariant (LTI), single input single output (SISO) system using asynchronous neuromorphic measurements from a DVS. Our approach goes directly from the events to control commands instead of first explicitly estimating the system states for feedback control. The intuition behind our approach is based on characterizing the lowest upper bound on the relative error between the continuous-time output that we do not have access to and the estimate of this output computed from the retinal events fired by the DVS. Then, by considering an auxiliary uncertain system, we show that an H_∞ controller stabilizes the auxiliary system and in turn stabilizes our hybrid system; furthermore, we derive the maximum event threshold that is required for a DVS to stabilize the given LTI system. Our solution is

⋆ Equal contribution from these authors.

[a] P. Singh, S.Z Yong, J. Gregoire, A. Censi and E. Frazzoli are with the Laboratory for Information and Decision Systems, Massachusetts Institute of Technology, Cambridge, MA, USA (e-mail: {prince1,szyong,jmmg,censi,frazzoli}@mit.edu).

facilitated with some ideas and tools drawn from works done within the context of control with limited information, in particular, the quantized control literature, e.g., [10]–[12].

Outline. This paper is organized as follows. In Section II, we clearly formulate the problem by first characterizing the DVS model and represent the combined LTI system and DVS model as a hybrid system. Then, in Section III, we design a stabilizing controller for this hybrid system. In turn, we present a criterion that provides us with the least restrictive (largest) event threshold that is required of a DVS to stabilize the given LTI system. In Section IV, we verify our results via a numerical experiment. Finally, in Section V, we present conclusions and outline possible extensions to this work.

II. Problem Formulation

LTI System. Consider the unstable, single input, stabilizable and detectable continuous-time LTI system (see Appendix I for a physical example) given by,

$$\begin{aligned} \dot{x} &= Ax + Bu, \\ y &= c'x, \end{aligned} \tag{1}$$

where $x \in \mathbb{R}^n$ is the system state, $u \in \mathbb{R}$ and $y \in \mathbb{R}$ are the scalar input and output, respectively, of the system, and $A \in \mathbb{R}^{n\times n}$, $\{B, c\} \in \mathbb{R}^{n\times 1}$. The initial state $x(0)$ is unknown. Note that we have no direct access to the output y, except through the "retinal event" measurements that we obtain from a neuromorphic camera, which we characterize next.

DVS Model. Our sensor of choice is the Dynamic Vision Sensor (DVS), which is the first commercially available neuromorphic sensor [2]. The DVS comprises of a photodiode that converts luminosity to a photocurrent, denoted by y as in (1), that is then amplified in a logarithmic fashion to detect brightness changes in real time. "Retinal events" are triggered when the brightness change exceeds a user-chosen threshold [1]; thus, we model the *trigger condition* based on which "retinal events" are generated by each pixel as

$$|\tau| \geq h, \tag{2}$$

where

$$\tau \triangleq \log_b |y| - \log_b |q| = \log_b |c'x| - \log_b |q|, \tag{3}$$

b is an arbitrary base, $q \in \mathbb{R}$ is the trigger reference (an internal state) and $h > 0$ is a user-defined event threshold. In the parlance of a hybrid system model, the trigger condition (2) is a guard set, which we denote as $\mathcal{D}$, i.e., a "retinal event" occurs when the combined system (LTI system and DVS model) state $\mathbf{x} := [x^\top, q]^\top \in \mathcal{D}$.

The k-th "retinal event" is then given by the triple: $\langle t_k, \langle x_p(t_k), y_p(t_k)\rangle, p(t_k)\rangle$, where t_k denotes the timestamp at which the "retinal event" was fired and $\langle x_p(t_k), y_p(t_k)\rangle$ represents the pixel coordinates where a "retinal event" was fired. However, in this paper, we will only discuss the single pixel case, hence we have a scalar output y in (1).

As aforementioned, we have no access to this output y, but instead we have access to polarity measurements, $p \in \{-1, 0, +1\}$ given by the events:

$$p = \begin{cases} \operatorname{sgn}(\tau), & \text{if } \mathbf{x} \in \mathcal{D}, \\ 0, & \text{otherwise.} \end{cases} \tag{4}$$

Thus, the (unobserved) evolution of the trigger reference is given by

$$q^+ = q\rho^{-p}, \tag{5}$$

where for convenience, we define

$$\rho \triangleq b^{-h} \in (0, 1), \tag{6}$$

as the spacing of the logarithmic partitions induced onto the output space by the logarithmic *trigger condition* in (2). This choice of ρ in (6) captures the range of positive values for the event threshold h of the DVS. Then, the *trigger condition* (2) can be equivalently re-written as

$$\mathcal{D} \triangleq \{\mathbf{x} : \left|\frac{c'x}{q}\right| \geq \frac{1}{\rho} \text{ or } \left|\frac{c'x}{q}\right| \leq \rho\}, \tag{7}$$

which explicitly defines our guard set $\mathcal{D}$ in terms of ρ.

Further, we make the following assumptions regarding the trigger reference q:

- (A1) The initial trigger reference $q(0)$ is known and lies in the interval $\rho \leq \left|\frac{c'x(0)}{q(0)}\right| \leq \frac{1}{\rho}$ with $y(0) = c'x(0) \in \mathcal{D}^c$, the complementary of the guard set $\mathcal{D}$.
- (A2) The sign of q is known at all times.

The former assumption may be restrictive, but one can typically calibrate the DVS, e.g., by initializing the DVS in an environment of known luminosity. The consideration of the case when the initial trigger reference $q(0)$ is known within a certain bound is a topic of future investigation. Intuitively, this assumption along with the continuity of the output trajectory imply that the event trigger for the DVS always takes place when equality holds for the trigger condition (2). This in turn makes it possible to keep track of the internal trigger reference at all times. The latter assumption is only necessary when considering the general LTI system. In practice, the luminosity is always positive.

Combined System. Next, combining the LTI system in (1) and the DVS model in (5) yields the following hybrid system:

$$\begin{aligned} \dot{\mathbf{x}} &= \begin{bmatrix} \dot{x} \\ \dot{q} \end{bmatrix} = \begin{bmatrix} Ax + Bu \\ 0 \end{bmatrix}, \quad \mathbf{x} \in \mathbb{R}^{n+1} \setminus \mathcal{D}, \\ \dot{\mathbf{x}}^+ &= \begin{bmatrix} x^+ \\ q^+ \end{bmatrix} = \begin{bmatrix} x \\ q\rho^{-p} \end{bmatrix}, \qquad \mathbf{x} \in \mathcal{D}, \end{aligned} \tag{8}$$

where the polarity measurement p is given in (4) and the guard set $\mathcal{D}$ in (7). The hybrid automaton that results is illustrated in Figure 1.

Now, the stabilizing control problem with the DVS reads:

Problem 1. *The* objective *of this paper is two-fold:*

1) *Design an appropriate feedback controller u that incorporates polarity measurement p given by a DVS to* quadratically *stabilize the hybrid system given in* (8)*.*
2) *For the stabilizing controller designed for Problem 1-1, find the least restrictive (largest) upper-bound on*

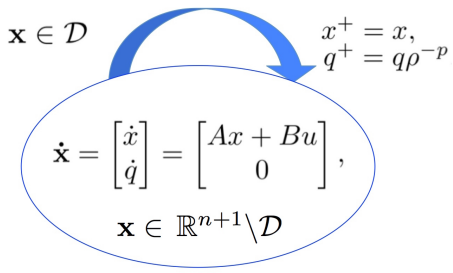

Fig. 1: Open loop hybrid automaton of combined LTI system and DVS model in (8), where $\mathcal{D}$ is given in (7).

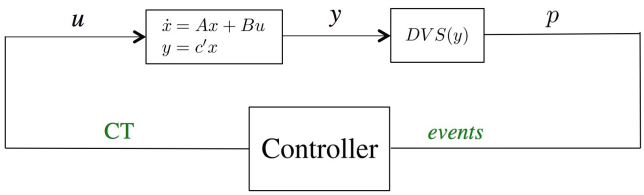

(a) Feedback controller in closed loop.

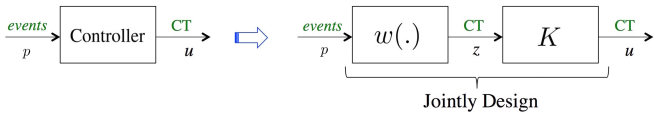

(b) Cascade decomposition of the feedback controller.

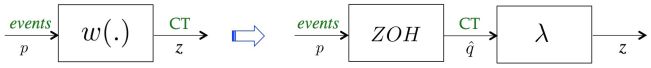

(c) Decomposition of $w(.)$ function.

Fig. 2: Controller design approach: From asynchronous events to continuous-time (CT) control commands.

> *the event threshold h^*, such that for any DVS with event threshold $h < h^*$, this controller quadratically stabilize the hybrid system in* (8).

III. Controller Design

In this work, we propose a controller that uses polarity measurements from the DVS in (4) to stabilize an LTI system (1). As shown in Figure 2(a), the LTI system outputs a continuous time signal y, which is broken down by the DVS to produce retinal events (i.e., based on the *trigger condition* in (2)). Our goal is to design a feedback controller that operates on the incoming events to generate a continuous time control signal u that would *quadratically* stabilize the pair (A, B).

The intuition behind our controller design is based on isolating the uncertainty in the polarity measurements of the DVS. Inspired by output feedback control, we construct an estimator $w(.)$ of the output signal y in Section III-A and use the resulting estimate z as an input to our controller K, which we will design in Section III-C. This cascade set-up of the feedback controller, which consists of the estimator $w(.)$ and the controller K is shown in Figure 2(b).

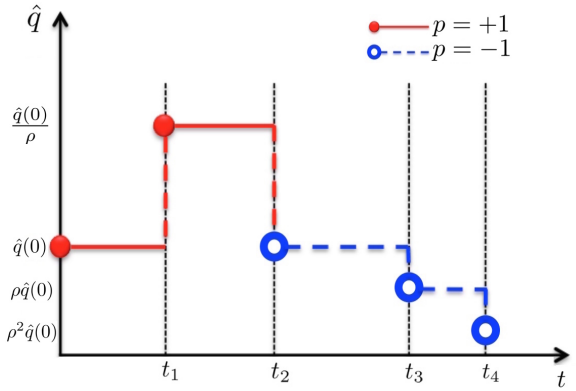

Fig. 3: Output of ZOH function (estimator of $\hat{q}$): red/solid dots indicate positive transitions while blue/hollow dots indicate negative transitions.

A. Design of estimator for y

Since there is no additional sensor to appropriately quantify the lack of information between the retinal events, a relatively simple design of $w(.)$ may be one that performs a Zero-Order-Hold (ZOH) on the retinal events arriving from the DVS that is then amplified by a non-zero scalar λ as shown in Figure 2(c). Thus, we will construct the signal z as an estimate of y with the following:

$$z \quad = \lambda \hat{q}, \quad 0 \neq \lambda \in \mathbb{R}, \tag{9}$$

where λ will be provided and justified in Section III-B, and $\hat{q}$ is an estimate of q. Since $q(0)$ is known according to (A1), we choose the estimate of the trigger reference q in view of the *trigger condition* in (2) to follow the same evolution of (5) as follows:

$$\hat{q}^+ = \hat{q}\rho^{-p}, \tag{10}$$

with $\hat{q}(0) = q(0)$. Thus, $\hat{q} = q$ for all t.

Figure 3 illustrates an example scenario for the evolution of (10), where the brightness increased (i.e., given by the red/solid dots) at the event-time t_1 from a known initial $\rho \leq y_0 \leq \frac{1}{\rho}$ and the brightness decreased (i.e., given by the blue/hollow dots) at event-times t_2, t_3, t_4.

B. Error quantification

Now, we would like to quantify the closeness of the designed continuous-time signal z to the unknown output y of the plant. More precisely, we would like to ascertain this closeness in the sense that the maximum absolute relative error $\left|\frac{z-y}{y}\right|$ is minimized. The closeness between z and y can be visualized using Figure 4; thus, we have the following lemma.

Lemma 1. *$\hat{q}$ estimates y with bounded (asymmetric) uncertainty:*

$$\rho y \leq \hat{q} = q \leq \frac{y}{\rho}. \tag{11}$$

Proof. By the construction of our estimate $\hat{q}$ in (10), $\hat{q}(0) = q(0)$ holds. Moreover, by Assumptions (A1) and (A2), and without loss of generality, q and y are assumed to be positive, we have that $\rho y \leq \hat{q} = q \leq \frac{y}{\rho}$ holds initially.

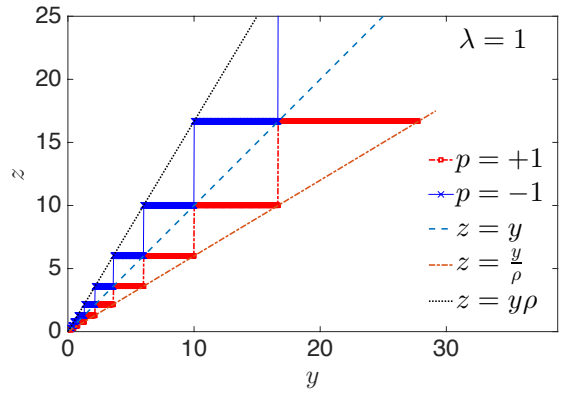

Fig. 4: Analysis of the signal z ($\lambda = 1$): Red/solid lines are due to positive transitions ($p = +1$) while blue/solid-star lines are due to negative transitions ($p = -1$).

At an arbitrary time t, assume that (11) holds. Then, until an event occurs, it still holds, as by definition of the trigger condition, we must have $\rho y < q = \hat{q} < \frac{y}{\rho}$. When an event occurs, before the transition, we have $y = \rho^{-p} q$ by definition of the trigger condition. After reset, we have $y^+ = y$ and $q^+ = \rho^{-p} q$. It follows that $\hat{q}^+ = q^+ = y^+$, so that $\rho y \leq \hat{q} = q \leq \frac{y}{\rho}$ holds after the transition.

By induction, $\rho y \leq \hat{q} = q \leq \frac{y}{\rho}$ holds at all times. ■

Note that Figure 4 has been generated with unit amplification, $\lambda = 1$, i.e., $z = \hat{q}$. We observe that the estimate $\hat{q}$ causes an unequal spacing between positive ($p = +1$) and negative ($p = -1$) transitions (note the unequal length of the blue and red segments). Furthermore, the logarithmic property of the *trigger condition* in (2) enables us to conservatively bound the error between the signals z and y via a sector whose borders are represented by the lines $z = \frac{y}{\rho}$ and $z = y\rho$. The ability to bound this error will facilitate the ensuing analysis in designing K in Section III-C. Furthermore, it is noteworthy that the uncertainty in our problem is similar but not equivalent to the uncertainties encountered in logarithmically quantized systems because of the 'overlap between partitions' that results from the possibility for positive and negative transitions.

The following provides us a symmetric bound on the absolute relative error between z and y signals; this symmetric bound is a desired trait as will be shown in Theorem 2.

Lemma 2. *The upper-bound δ_{HM} on the absolute relative error between the z and y signals is given by,*

$$\left| \frac{z - y}{y} \right| \leq \delta_{HM},$$

with

$$z = \lambda_{HM} \hat{q},$$

where $\delta_{HM} \triangleq \frac{1-\rho^2}{1+\rho^2}$ and $\lambda_{HM} \triangleq \frac{2\rho}{1+\rho^2}$.

Proof. By Lemma 1,

$$\rho y \leq \hat{q} \leq \frac{y}{\rho},$$

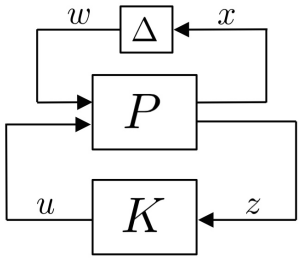

Fig. 5: H_∞ control problem with generalized plant P and controller K given in (14) and (15), respectively.

$$\frac{2\rho^2}{1+\rho^2} y \leq z = \lambda_{HM} \hat{q} = \frac{2\rho}{1+\rho^2} \hat{q} \leq \frac{2\rho}{\rho(1+\rho^2)} y,$$

$$(1 - \frac{1-\rho^2}{1+\rho^2}) y \leq z \leq (1 + \frac{1-\rho^2}{1+\rho^2}) y,$$

$$(1 - \delta_{HM}) y \leq z \leq (1 + \delta_{HM}) y,$$

which is a symmetric inequality and in turn gives an upper-bound on the relative error between z and y. ■

Additionally, it may be interesting to note that the amplification factor λ_{HM} is the harmonic mean (HM) of ρ and $\frac{1}{\rho}$ (i.e., the bounds of the trigger condition).

C. Design of K

Let us now note that the direct synthesis of a stabilizing controller for the hybrid system (8) may be difficult. Hence, to solve Problem 1-1, we resort to finding sufficient conditions for stabilizing the hybrid system by considering the stability of an auxiliary uncertain system, as stated in the following proposition.

Proposition 1. *The hybrid system* (8) *(with (A, B, c') stabilizable, detectable and $\rho \in (0, 1)$) is quadratically stable via a controller K if the following auxiliary uncertain system*

$$\begin{aligned} \dot{x} &= Ax + Bu, \\ z &= (1 + \Delta) c' x, \ |\Delta| \leq \delta_{HM} \end{aligned} \tag{12}$$

is quadratically stabilizable via the controller K with δ_{HM} given in Lemma 2.

Proof. Lemma 2 shows that the hybrid system (8) is an instance of the auxiliary uncertain system (12). Thus, the proposition holds directly. ■

We are now ready to state the solution to Problem 1-1 in the following theorem.

Theorem 1. *The hybrid system* (8) *(with (A, B, c') stabilizable, detectable and $\rho \in (0, 1)$) is quadratically stable via an H_∞ controller, provided that the event threshold h in* (2) *for the DVS is upper-bounded, i.e.,*

$$h < h^\star = \log_b \sqrt{\tfrac{\gamma+1}{\gamma-1}}, \tag{13}$$

where $\gamma > 1$ is the H_∞ norm of the closed-loop uncertain system (12) *with $\delta_{HM} = \frac{1-\rho^2}{1+\rho^2}$.*

Proof. We will show that the auxiliary uncertain system (12) can be quadratically stabilized with an H_∞ controller in conjunction with small gain theorem.

Let us cast this problem as a standard H_∞ control problem shown in Figure 5 with the generalized plant P given by

$$P = \left[\begin{array}{c|cc} A & 0_{n\times n} & B \\ \hline I_{n\times n} & 0_{n\times n} & 0_{n\times 1} \\ c' & c' & 0_{1\times 1} \end{array}\right] \tag{14}$$

and the H_∞ controller K given by

$$K = \left[\begin{array}{c|c} A_c & B_c \\ \hline C_c & D_c \end{array}\right] \tag{15}$$

with input z from Lemma 2 that can be synthesized under some mild assumptions given in [13]. Furthermore, we will obtain the gain γ of the resulting closed-loop system (P, K) in Figure 5. This gain γ can be found via a γ-iteration algorithm [13] as $||T_{xw}(s)||_{H_\infty} < \gamma$ where $T_{xw}(s)$ is transfer function from w to x.

Then, applying the small gain theorem, with $|\Delta| \leq \delta_{HM}$, we find an upper bound on δ_{HM} that can be tolerated, i.e.,

$$\delta_{HM} < \delta^*_{HM} \triangleq \frac{1}{\gamma},$$

such that the closed loop system (P, K, Δ) is quadratically stable or equivalently robustly asymptotically stable [14]. Now, in view of $\delta_{HM} = \frac{1-\rho^2}{1+\rho^2}$ from Lemma 2, we obtain $\rho^* = \sqrt{\frac{\gamma-1}{\gamma+1}}$. Additionally, from our definition of ρ in (6), we obtain an upper bound on the tolerable event threshold

$$h < h^\star \triangleq \log_b \sqrt{\frac{\gamma+1}{\gamma-1}}.$$

Finally, by Proposition 1, the H_∞ controller also quadratically stabilizes the hybrid system (8). ■

In Lemma 2, we reasoned that the minimization of the relative error between z and y would result in the largest h^*, by having symmetric error bounds on z via a choice of $\lambda_{HM} = \frac{2\rho}{1+\rho^2}$. However, this reasoning needs verification. For the H_∞ controller that we found in Theorem 1, we verify in the following theorem that the threshold h^* in Theorem 1 indeed solves Problem 1-2.

Theorem 2. *The choice of $\lambda_{HM} = \frac{2\rho}{1+\rho^2}$ in Lemma 2 yields the least restrictive (largest) upper bound on the event threshold h^* in Theorem 1.*

Proof. The problem of finding the least restrictive upper bound on the event-threshold, h^*, in (13) for the DVS is equivalent to finding the minimum ρ^*, and can be cast as the following optimization problem:

$$\begin{aligned} \underset{\rho,\lambda}{\text{minimize}} \quad & \rho, \\ \text{subject to} \quad & 0 < \rho < 1, \\ & \delta = \max\{1-\lambda\rho, \frac{\lambda}{\rho} - 1\}, \\ & 0 < \delta \leq \bar{\delta}, \end{aligned}$$

with a $\bar{\delta}$ that satisfies the small gain theorem, i.e., $\bar{\delta}\gamma < 1$, as in Theorem 1. To solve this optimization problem

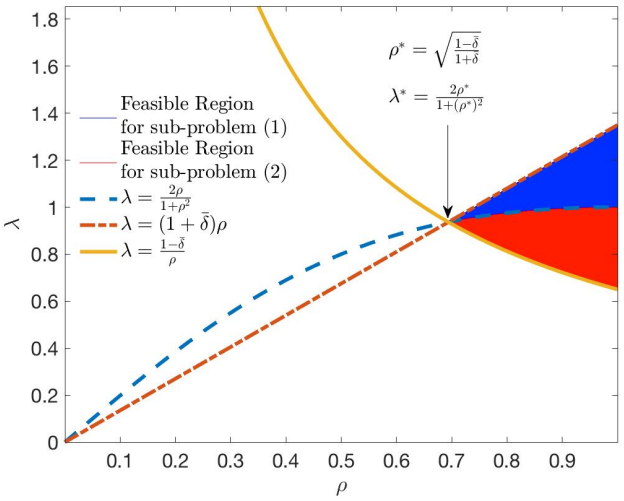

Fig. 6: Illustration of the optimization problem for finding (ρ^*, λ^*) via two sub-problems (with $\bar{\delta} = 0.35$).

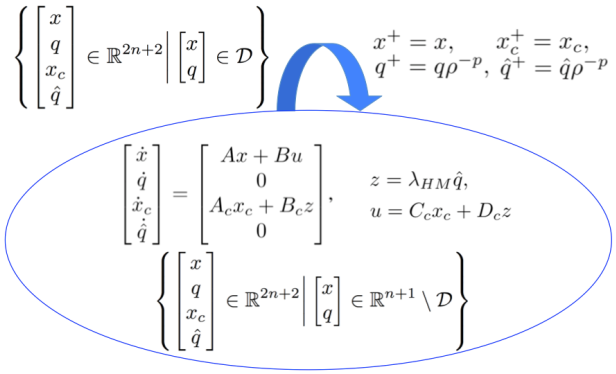

Fig. 7: Closed loop hybrid automaton of combined LTI system, DVS model and H_∞ controller, where τ and $\mathcal{D}$ are given in (3) and (7), respectively, and with $h < h^*$ in Theorem 1.

analytically, we note that ρ^* is given by $\min\{\rho_1, \rho_2\}$ in view of the following two sub-problems (cf. Figure 6):

$$\begin{aligned} \underset{\rho_1,\lambda_1}{\text{minimize}} \quad & \rho_1, \\ \text{subject to} \quad & 0 < \rho_1 < 1, \\ & \frac{2\rho_1}{1+\rho_1^2} \leq \lambda_1, \\ & \rho_1 < \lambda_1 \leq \rho_1(\bar{\delta}+1), \end{aligned} \qquad \begin{aligned} \underset{\rho_2,\lambda_2}{\text{minimize}} \quad & \rho_2, \\ \text{subject to} \quad & 0 < \rho_2 < 1, \\ & \frac{2\rho_2}{1+\rho_2^2} \geq \lambda_2, \\ & \frac{1-\bar{\delta}}{\rho_2} < \lambda_2 \leq \frac{1}{\rho_2}. \end{aligned}$$

It can be verified that the solutions to both sub-problems coincide in a unique $\lambda^* = \lambda_{HM}(\rho^*)$, as illustrated in Figure 6. Thus, this concludes the proof since ρ^* results in the least restrictive upper bound h^* in view of (6). ■

To sum up, our resulting closed loop hybrid automaton is illustrated in Figure 7.

D. Practical Stability

A potential problem that can arise in the practical implementation of our approach is the possibility of having an

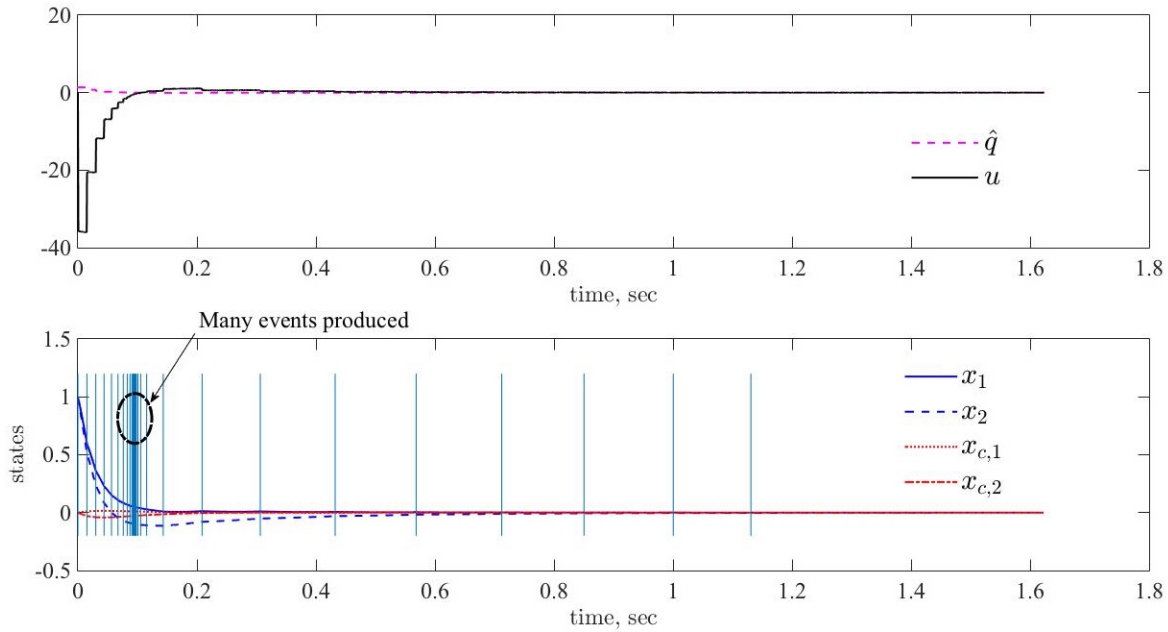

Fig. 8: Numerical Example: Stabilization of unstable system. The top plot shows the estimate of the trigger reference and the control command, while the bottom plot shows the evolution of closed loop system dynamics.

infinite number of events when the output is near the origin. This can occur due to the logarithmic *trigger condition* in (2), which induces logarithmic spacings separated by ρ in the output space that carry over to the state-space due to the linearity of the output y. In particular, when the output y crosses 0, an infinite number of events would be fired by the DVS over a finite time interval (similar to a Zeno phenomenon observed in hybrid systems, e.g., in [15]), making it impractical for any controller to keep up with in real time.

To overcome this potential problem, we propose the inclusion of an auxiliary band near the origin as in [16]. Thus, instead of requiring quadratic stability, we require that the states instead converge to a neighborhood of the origin (i.e., *practical* stability) as defined in [10]. We remark that this problem would not happen for vision sensors as luminosity is nonnegative.

IV. Numerical Experiment

In this section, we demonstrate our proposed approach in Section III-C with the following unstable, but stabilizable and detectable, LTI system:

$$A = \begin{bmatrix} 2 & 10 \\ 0 & 5 \end{bmatrix}, \quad B = \begin{bmatrix} 1 \\ 1 \end{bmatrix}, \quad c = \frac{1}{\sqrt{5}} \begin{bmatrix} 2 \\ 1 \end{bmatrix}.$$

From the design of an H_∞ controller for the auxiliary uncertain system in (12) using the `hinfric` command in MATLAB, we obtain $\gamma = 1.3867$ and $h^* = 0.9100$. The simulation results are presented in Figure 8. The bottom plot shows that the controller indeed stabilizes the plant and there are many events produced when the output of the system crosses the origin for the reasons discussed in Section III-D. We have included an auxiliary band with width 10^{-4} near the origin. When no more events are produced for some time (i.e., the states oscillate strictly within the band), then, we have practical stability, which occurs at around 1.62 seconds.

V. Conclusions and Future Work

The Dynamic Vision Sensor (DVS) is a neuromorphic sensor, which is a recent addition to the classes of vision sensors. The nice properties of the DVS promise to facilitate agile robotic maneuvers. However, existing vision algorithms cannot be directly adapted to process these events; thus, new algorithms need to be developed.

In this work, we proposed an H_∞ controller that *quadratically* stabilizes LTI systems using DVS measurements. In particular, we provide the least restrictive upper bound on the event threshold, h^*, for the DVS such that the pair (A, B) is *quadratically* stabilized. This work can be viewed as an initial attempt to locally stabilize a nonlinear system about some operating point using DVS measurements.

There are many interesting directions of future research. An important one is to develop a control scheme that can stabilize a given LTI system in the presence of non-deterministic trigger reference. Additionally, a linear varying luminance profile may not be regularly encountered in practice and so a control scheme needs to be developed that can handle an accurate description of the environment's luminance, e.g., through an integrative sensor model. Finally, it would be crucial to generalize the results for multiple input multiple output (MIMO) systems to tackle real world applications.

Acknowledgments

This work was supported by the Singapore National Research Foundation through the SMART Future Urban Mobility project.

REFERENCES

[1] Shih-Chii Liu and Tobi Delbruck. Neuromorphic sensory systems. *Current opinion in neurobiology*, 20(3):288–295, 2010.

[2] Patrick Lichtsteiner, Christoph Posch, and Tobi Delbruck. A 128×128 120 db 15 μs latency asynchronous temporal contrast vision sensor. *Solid-State Circuits, IEEE Journal of*, 43(2):566–576, 2008.

[3] Sawyer B Fuller, Michael Karpelson, Andrea Censi, Kevin Y Ma, and Robert J Wood. Controlling free flight of a robotic fly using an onboard vision sensor inspired by insect ocelli. *Journal of The Royal Society Interface*, 11(97):20140281, 2014.

[4] Andrew J Barry and Russ Tedrake. Pushbroom stereo for high-speed navigation in cluttered environments. In *Robotics and Automation (ICRA), 2015 IEEE International Conference on*, pages 3046–3052. IEEE, 2015.

[5] Jörg Conradt, Matthew Cook, Raphael Berner, Patrick Lichtsteiner, Rodney J Douglas, and T Delbruck. A pencil balancing robot using a pair of aer dynamic vision sensors. In *Circuits and Systems, 2009. ISCAS 2009. IEEE International Symposium on*, pages 781–784. IEEE, 2009.

[6] Tobi Delbruck and Manuel Lang. Robotic goalie with 3 ms reaction time at 4% cpu load using event-based dynamic vision sensor. *Neuromorphic Engineering Systems and Applications*, page 16, 2015.

[7] Erich Mueller. *Feedback Control of Dynamic Systems with Neuromorphic Vision Sensors*. PhD thesis, Massachusetts Institute Of Technology, October 2015.

[8] Andrea Censi. Efficient neuromorphic optomotor heading regulation. In *American Control Conference (ACC), 2015*, pages 3854–3861. IEEE, 2015.

[9] Karl J Aström. Event based control. In *Analysis and design of nonlinear control systems*, pages 127–147. Springer, 2008.

[10] Nicola Elia and Sanjoy K Mitter. Stabilization of linear systems with limited information. *Automatic Control, IEEE Transactions on*, 46(9):1384–1400, 2001.

[11] Minyue Fu and Lihua Xie. The sector bound approach to quantized feedback control. *Automatic Control, IEEE Transactions on*, 50(11):1698–1711, 2005.

[12] Linh Vu and Daniel Liberzon. Stabilizing uncertain systems with dynamic quantization. In *Decision and Control, 2008. CDC 2008. 47th IEEE Conference on*, pages 4681–4686. IEEE, 2008.

[13] John C Doyle, Keith Glover, Pramod P Khargonekar, and Bruce A Francis. State-space solutions to standard H_2 and H_∞ control problems. *Automatic Control, IEEE Transactions on*, 34(8):831–847, 1989.

[14] Andy Packard and John Doyle. Quadratic stability with real and complex perturbations. *Automatic Control, IEEE Transactions on*, 35(2):198–201, 1990.

[15] Rafal Goebel, Ricardo G Sanfelice, and Andrew Teel. Hybrid dynamical systems. *IEEE Control Systems Magazine*, 29(2):28–93, April 2009.

[16] Bruno Picasso and Antonio Bicchi. Hypercubes are minimal controlled invariants for discrete-time linear systems with quantized scalar input. *Nonlinear Analysis: Hybrid Systems*, 2(3):706–720, 2008.

APPENDIX I
PHYSICAL EXAMPLE

Figure 9 presents a physical example that may be encountered in practice. In this example, the DVS is mounted on a platform with linear (x_1, x_2) dynamics and looks at a linearly varying brightness profile whose gradient is given by the linearized sensor function, c. The H_∞ controller developed in Section III-C for each pixel of the DVS produces suitable control commands u to the platform for moving the DVS to the point with lowest luminosity.

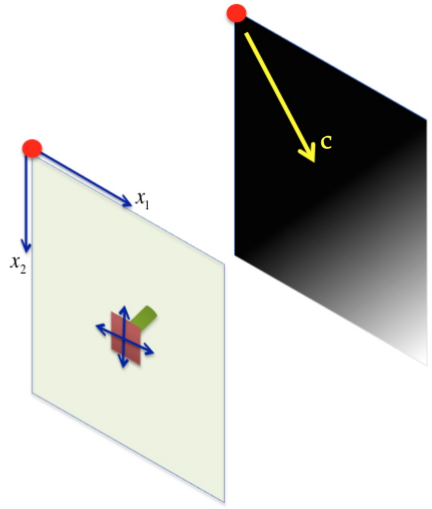

Fig. 9: Physical example: DVS (green cylinder) mounted on a platform with linear (x_1, x_2) dynamics and facing a linearly varying brightness profile. The DVS provides control commands u to the platform to move the camera towards the red dot (with lowest luminosity).